

## Effects of Chloride and pH on Passivation Characteristics of Q235 Steel in Simulated Concrete Pore Solution

Lupeng Liu<sup>1</sup>, Senlin Li<sup>2</sup>, Zhiming Gao<sup>1,\*</sup>, Hang Jia<sup>1</sup>, Ye Wu<sup>2</sup>, Wenbin Hu<sup>1</sup>

<sup>1</sup> Tianjin Key Laboratory of Composite & Functional Materials, School of Materials Science and Engineering, Tianjin University, Tianjin 300350, China;

<sup>2</sup> Nanjing Hydraulic Research Institute, Nanjing 210029, China

\*E-mail: [gaozhiming@tju.edu.cn](mailto:gaozhiming@tju.edu.cn)

Received: 4 March 2022 / Accepted: 11 April 2022 / Published: 7 May 2022

---

The impact of chloride and pH on the passivation and corrosion behavior of Q235 steel in simulated concrete pore solutions was studied by different electrochemical methods. Mott-Schottky test results demonstrated that the passive film of Q235 steel showed n-type semiconductor behavior, with two different donor densities at pH 13. As the chloride concentration is increased the donor density is also elevated, resulting in elevated disorder and number of impurities present in the passive film. The electrochemical impedance spectroscopy results indicated that as the chloride concentration was increased the electric double layer capacitance also increased and the charge transfer resistance decreased. This was indicative of the corrosion resistance properties of the passive film decreasing. As the pH value is reduced the passive film will undergo corrosion at lower chloride concentrations, with the passive film becoming more susceptible to corrosion. A highly alkaline solution can provide better protection for steel in the presence of chloride.

---

**Keyword:** Q235 steel; passive film; EIS; Mott-schottky analysis; Corrosion.

### 1. INTRODUCTION

Reinforced concrete is used worldwide across the construction industry for numerous applications. The corrosion of reinforced concrete is one of the key characteristics that is considered when determining the stability of a reinforced concrete structure [1]. The corrosion of reinforced concrete is an electrochemical process, which depends upon the surface conductivity between the concrete and the steel used for reinforcement. The concentration of dissolved oxygen in pore solution near the reinforcement is a key variable that needs to be considered in these systems [2]. For various applications, both low and medium carbon steels make up a large proportion of the material used for

concrete reinforcement. The key chemical reaction that influences corrosion is the hydration of cement. This reaction will form a highly alkaline solution with a pH that ranges between 12.5 and 13.6. Under these conditions, the steel used for reinforcement will often form a surface layer that has excellent corrosion resistance properties [3,4]. This protective film, although very thin, has strong adhesion and chemical stability under alkaline conditions. The passive film also greatly reduces the ionic mobility between steel and the surrounding concrete, reducing the rate of corrosion. The stability of the passive film is closely related to the pH value of the fluid in the concrete micro-environment. Previous studies suggest that when the pH value is less than 9.8, a passive film will not form on the steel reinforcement. When the pH value is between 9.8 and 11.5, the film is unstable and cannot completely prevent corrosion of the steel. When the pH value is greater than 11.5, the steel reinforcement is completely passivated [5]. As reinforced concrete structures will be exposed to various environmental conditions, any structural problems are a significant social and public safety concern, with additional impacts on construction project economics [6,7]. The penetration of chloride and the carbonization of concrete are the two primary mechanisms leading to the corrosion of the passive film on steel [8,9]. As concrete is a porous structure, when there are corrosive compounds or ions in the local environment, these erosive agents can penetrate and destroy the passive film on the steel reinforcement. Chloride is one of the most important erosive ions, primarily due to widespread use for deicing salts and its presence in marine environments [10]. The presence of chloride can cause local breakdown of the passive film and expose the metal to these environmental conditions. Chloride will compete with the hydroxide ions needed to form the passive layer, generating soluble and unstable compounds that cause the metal to dissolve further. Carbon dioxide can also diffuse through pores in the concrete leading to a decrease in the solution alkalinity. As a result of the carbon diffusion, the pH can be reduced as low as 9, leading to a significant reduction in the protective effect of the passive film [11]. Carbonization often occurs during the process of chloride transfer, affecting diffusion which is of great significance to the study of their interaction [12].

Various studies have investigated the corrosion of steel in simulated concrete pore solutions (SCPS). SCPS will reproduce the chemical environment in concrete and shorten the test period, providing rapid, high quality results for the study of cement-based materials. The thermodynamic properties at the interface between steel and SCPS are similar to those expected at the interface between steel and concrete. It is expected that immersion of reinforcement material in SCPS to study passive film formation or degradation is consistent with the results that are observed in the steel-concrete system.

In this study, the passive film performance and corrosion behavior of Q235 steel in SCPS at different chloride concentrations and pH value were studied using different electrochemical test methods. These included polarization curve analysis, electrochemical impedance spectroscopy (EIS) and Mott-Schottky analysis.

## 2. MATERIALS AND METHODS

Q235 steel was processed into 1cm×1cm×0.3cm sample in the experiment. The back of the sample was welded with copper wire and sealed with PVC pipe and epoxy resin. The exposed area was

1cm<sup>2</sup>, which was used as the working electrode. Specimens were polished sequentially with 80, 150, 400, 800, 1500 and 3000# sandpaper, before been placed in anhydrous ethanol for ultrasonic cleaning. After rinsing with deionized water and anhydrous ethanol the samples were placed in a dish for drying before use. The SCPS were prepared using NaOH, with the pH adjusted to 9, 11, 12.5 or 13. NaCl was used to adjust to the different chloride concentrations tested.

A three-electrode system was used for electrochemical testing, with a saturated calomel electrode (SCE) used as the reference electrode and Pt sheet used as the auxiliary electrode. A Parstat 2273 electrochemical workstation was used for the test. Q235 steel was immersed in SCPS and electrochemical tests were conducted after immersion in solution for 3 hours to ensure that the passive film was stabilized. Mott-Schottky tests were performed at a frequency of 1000 Hz with a potential step of 50 mV from -0.9 to 0.6 V<sub>SCE</sub>. Scanning was conducted from low to high potential. During EIS measurements the scanning frequency of the test parameters was 100kHz to 10mHz using a small sinusoidal voltage signal of 10 mV peak-to-peak around the OCP. The data obtained after the test was fitted by Zsimpwin software. The anodic potentiodynamic polarization sweep rate was 0.5 mV/s in the anodic direction, from -150 mV versus the OCP.

### 3. RESULTS AND DISCUSSION

#### 3.1 Mott-Schottky Analysis

The Mott-Schottky plots of Q235 carbon steel immersed for three hours in SCPS at different chloride and pH values is presented in Figure 1. A positive slope was calculated, ranging from -0.6 to 0.5V<sub>SCE</sub>, indicative that the passive film is behaving as a typical n-type semiconductor. This potential range corresponds to the depletion layer of the passive film. According to the M-S equation, the charge carrier located in the space charge layer are electrons, with the impurity state of the passive film being the donor state. After the majority of free charge carriers are generated via excitation, the newly formed depletion layer showed a strong positive charge from oxidation of the donor state [13]. The flat band potential was approximately -0.6V<sub>SCE</sub> at low chloride concentrations and -0.65V<sub>SCE</sub> at elevated concentrations. When the potential value is lower than the flat band potential, it corresponds to the enrichment layer of passive film. When the capacitor increases, the passive film enters the inversion layer. The donor concentration  $N_D$  of the passive film was calculated using the M-S equation(Eq.1) :

$$N_D = \frac{2}{e\epsilon_r\epsilon_0 S} (1)$$

Where S is the slope of the Mott-Schottky plot, e is the electronic charge ( $1.602 \times 10^{-19} \text{C}$ ),  $\epsilon_0$  is the permittivity of free space ( $8.854 \times 10^{-12} \text{F} \cdot \text{m}^{-1}$ ) and  $\epsilon_r$  is the relative permittivity. When assuming iron oxide as the steel surface passive film, the relative permittivity is 12 [14]. For a purely n-type semiconductor with a single donor state, the M-S plot should correspond to a single positive slope [15]. However, the slope changed when the potential reached 0.1-0.2 V during test work at pH 13, which was attributed to a second donor state located deep in the band gap of the steel oxide film [16]. This is in addition to the characteristic shallow donor state of n-type semiconductors that are fully ionized. For iron-based alloys, the shallow and deep donor states are attributed to the oxidation of Fe from the

tetrahedral and octahedral sites in the oxide lattice, respectively [17]. In the initial stages of passivation, both tetrahedral and octahedral sites are from Fe(II) oxides. As the period of passivation increases, the Fe(III) oxides occupying the octahedral sites will begin to contribute to the passive film as the outer structure [18]. In comparison to octahedral sites, ionization at tetrahedral sites occurs more readily and at lower applied potentials due to reduced bond energies. The donor concentration  $N_D$  of the passive film was calculated from the curve near the open circuit potential. The calculation results are reported in Table 1. The slope of the Mott-Schottky plots decreases and the donor density  $N_D$  increases as the chloride concentration is increased. The flat band potential shifts negatively and the corrosion resistance of the passive film is also measured to decrease gradually.

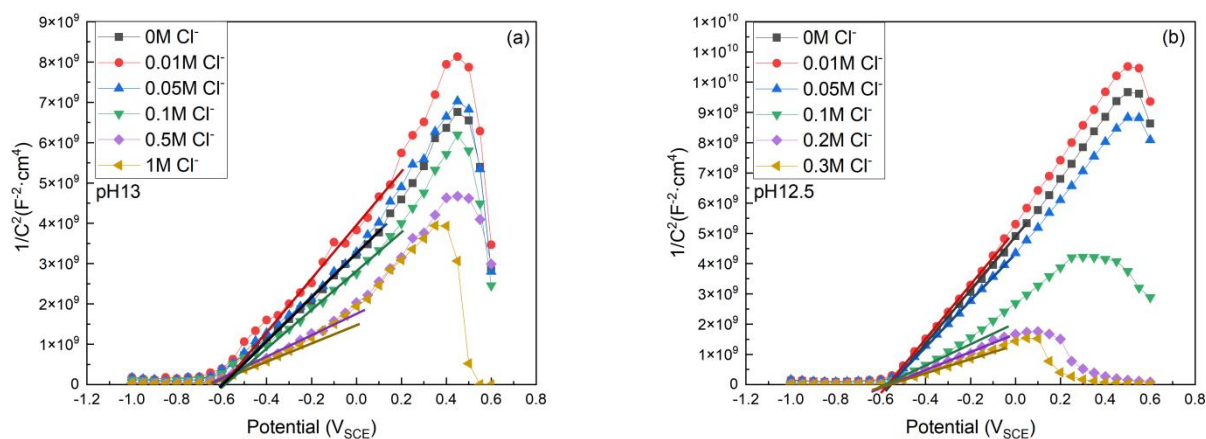


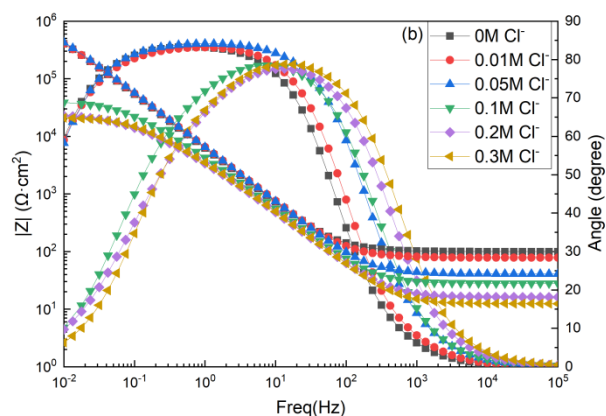
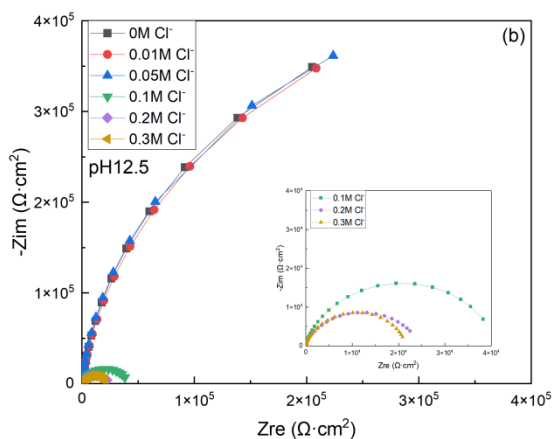
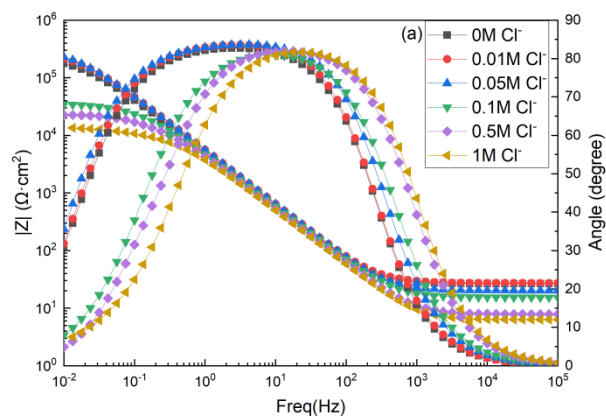
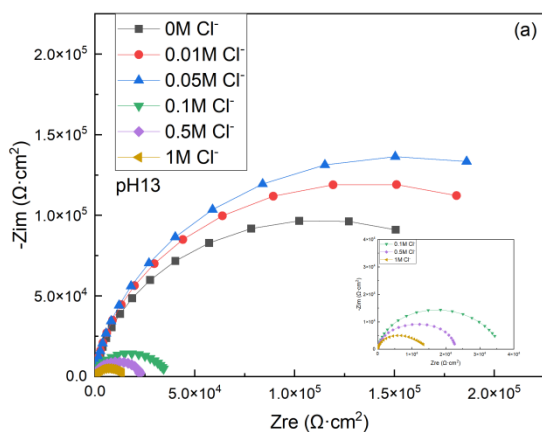
**Figure 1.** Mott-Schottky results of Q235 carbon steel in the SCPS with different chloride concentrations and different pH value after 3 hours of immersion (a) pH13, (b) pH12.5.

**Table 1.**  $N_D$  of the passive film on Q235 steel in the SCPS with different chloride concentrations and different pH after 3h of immersion.

pH	Cl <sup>-</sup> (M)	$N_D$ ( $10^{21} \text{ cm}^{-3}$ )
13	0	2.15
	0.01	1.77
	0.05	2.17
	0.1	2.44
	0.5	4.44
	1	5.20
12.5	0	1.33
	0.01	1.31
	0.05	1.52
	0.1	3.36
	0.2	3.96
	0.3	5.05

The addition of chloride may increase the quantity of impurities incorporated into the passive film, resulting in an increase of the capacitance of the space charge layer. The passive film has a high concentration of various point defects, such as metal and oxygen vacancy, which act as the electron donors for n-type semiconductors. When chloride at the interface of the passive film are absorbed into oxygen vacancies, oxygen vacancy/metal ions pairs are generated by the reaction. The oxygen vacancy continues to react with anions present perpetuating the generation of additional metal vacancies. The metal vacancy can pass through the passive film layer to reach the interface between the film and the metal substrate. If the diffusion rate is too fast, it will cause the metal vacancy to accumulate at the interface between the film and metal. The passive film may be thinned or partially detached from the metal surface[19]. Consequently, the higher the donor concentration is, the more likely that the metal vacancy enrichment occurs at the interface between passive film and metal. This will result in the poor stability of a passive film when exposed to solution. Chloride will also adsorb at defects in the passive film structure. When the concentration of chloride reaches a critical threshold, it can replace hydroxide ions at the surface of the steel, inhibiting and minimizing the formation of additional passive film [20].

### 3.2 EIS



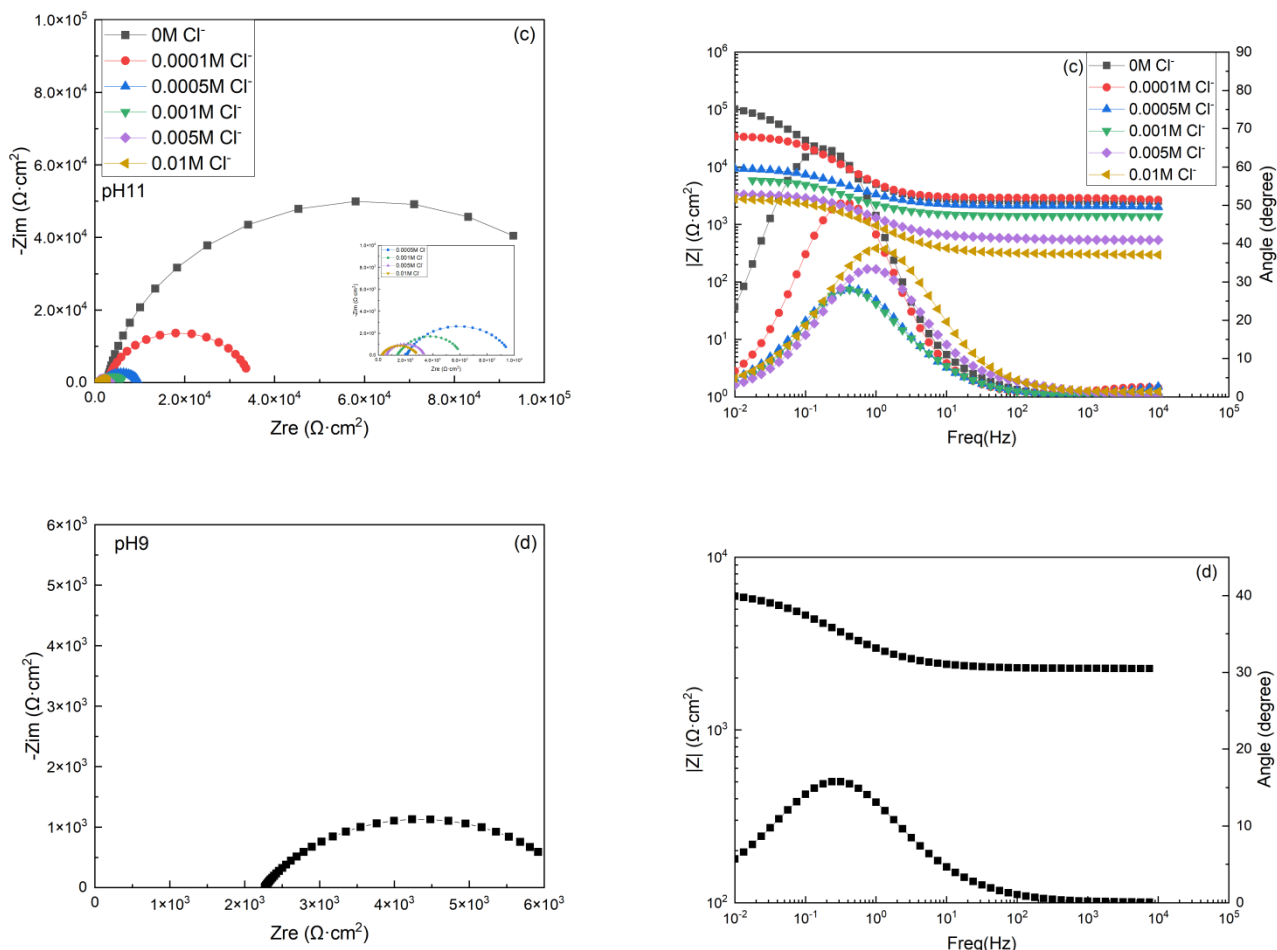


**Figure 2.** EIS results of Q235 carbon steel in the SCPS with different chloride concentrations and different pH value after 3 hours of immersion (a) pH13, (b) pH12.5, (c) pH11, (d) pH9.

Nyquist and Bode plots of Q235 carbon steel immersed for three hours in SCPS at different chloride and pH values are presented in Figure 2. Fitting by Zsimpwin software, the equivalent circuit is shown in Fig. 3, where  $R_s$  represents solution resistance,  $Q_f$  represents the constant phase element of passive film or corrosion product,  $R_f$  represents the resistance of passive film or corrosion product,  $Q_{dl}$  represents the constant phase element of the double electric layer at the steel interface and  $R_{ct}$  represents the charge transfer resistance. The high-frequency time constants,  $R_f$  and  $Q_f$ , are related to the formation of passive films and corrosion products. The low-frequency time constants,  $R_{ct}$  and  $Q_{dl}$ , reflect the charge transfer process of the steel. A constant phase element (CPE, denoted as  $Q$ ) was used instead of the pure capacitance  $C$  to represent the inhomogeneity of the steel surface. The inhomogeneity is primarily caused by non-uniform thickness of the passive film, the presence of defects in the passive film, the formation of corrosion pits and the precipitation of corrosion products [21]. The results obtained by fitting are shown in Table 2. At pH 12 and 13 when the chloride concentration is less than 0.05M, the values for  $R_{ct}$  do not change significantly. As the chloride concentration increases to 0.1M, the  $R_{ct}$  was reduced and  $Q_f$  and  $Q_{dl}$  increased significantly. At pH 11, when the chloride concentration was increased to 0.0001 and 0.0005M, the  $R_{ct}$  value was significantly reduced and the values of  $Q_f$  and  $Q_{dl}$  increased.

When chloride reaches a critical concentration, the  $R_{ct}$  value will be decreased significantly due to breakdown of passive film, resulting in local corrosion. During the corrosion process, loose corrosion products will be formed on the steel surface, and the increase of  $Q_f$  is caused by the formation of a loose and porous rust layer[22]. The increase in the  $Q_{dl}$  value is due to the thinning or cracking of the passive film and the pitting corrosion caused by chloride resulting in surface porosity[23]. At pH 9, Q235 steel was unable to form a passive film and has no protective effect. As the pH is decreased further the passive film will corrode at lower chloride concentration. In comparison, a highly alkaline solution will provide better protection.

**Table 2.** EC parameters for Q235 steel in the SCPS with different chloride concentrations and different pH value after 3 hours of immersion.

pH	Cl <sup>-</sup> (M)	$R_s$ ( $\Omega \cdot \text{cm}^2$ )	$Q_f$ ( $\mu\text{F} \cdot \text{cm}^{-2}$ )	$n_1$	$R_f$ ( $\Omega \cdot \text{cm}^2$ )	$Q_{dl}$ ( $\mu\text{F} \cdot \text{cm}^{-2}$ )	$n_2$	$R_{ct}$ ( $\Omega \cdot \text{cm}^2$ )
13	0	26.43	16.68	1	28.15	19.76	0.8514	$2.246 \times 10^5$
	0.01	27.26	16.19	1	31.76	15.96	0.8558	$2.736 \times 10^5$
	0.05	20.25	15.80	1	21.87	17.03	0.8565	$3.131 \times 10^5$
	0.1	15.28	37.03	0.9287	$2.773 \times 10^4$	184.9	0.7085	$9.018 \times 10^3$
	0.5	7.836	39.42	0.9367	$1.814 \times 10^4$	307.3	1	$4.741 \times 10^3$
	1	6.302	40.25	0.9411	$8.352 \times 10^3$	181.9	0.4742	$7.004 \times 10^3$
12.5	0	99.94	25.65	0.9308	256.8	3.045	1	$9.616 \times 10^5$
	0.01	78.41	11.78	1	41.89	15.94	0.8788	$9.962 \times 10^5$
	0.05	40.39	23.33	0.9314	58.26	3.967	1	$9.446 \times 10^5$
	0.1	28.00	39.78	0.9209	$1.809 \times 10^4$	41.32	0.7592	$2.339 \times 10^4$
	0.2	16.16	46.29	0.9166	$8.048 \times 10^3$	61.94	0.6468	$1.683 \times 10^4$
	0.3	12.41	44.13	0.9215	$8.950 \times 10^3$	49.89	0.7836	$1.265 \times 10^4$
11	0	3305	12.1	0.8791	3560	22.71	0.9390	$1.149 \times 10^5$
	0.0001	2802	29.2	0.9397	2007	24.27	0.9151	$2.941 \times 10^4$
	0.0005	1964	68.08	0.9952	1703	128.3	0.7634	$7.549 \times 10^3$
	0.001	1498	115.6	0.9548	1484	114.1	0.9317	$3.237 \times 10^3$
	0.005	479.1	162.4	0.7652	1063	217.7	0.7820	$2.879 \times 10^3$
	0.01	279.9	90.5	0.9300	390.1	363.5	0.7831	$2.500 \times 10^3$

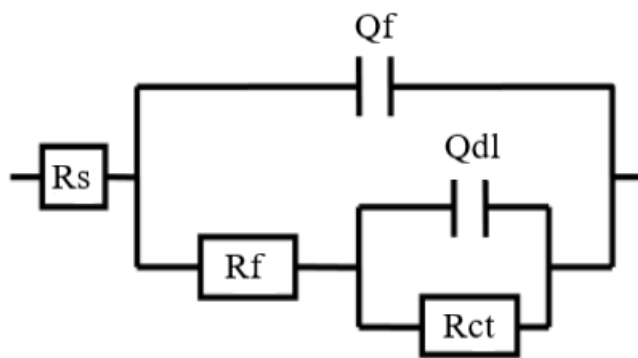


**Figure 3.** Equivalent circuit of EIS

## 3.3 Potentiodynamic polarization curves

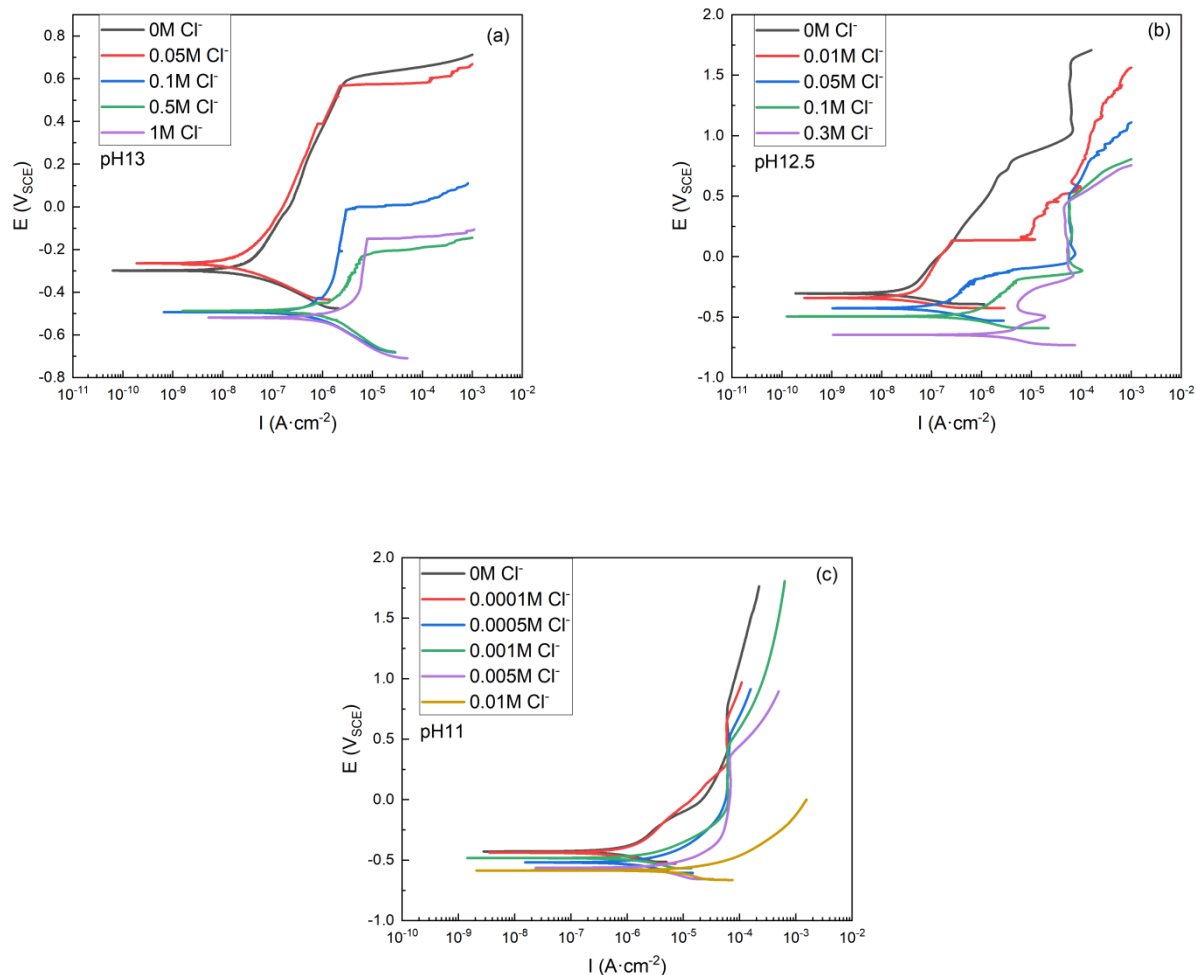


**Figure 4.** Potentiodynamic polarization performance of Q235 steel in the SCPS with different chloride concentrations and different pH value after 3 hours of immersion (a) pH13, (b) pH12.5, (c) pH11.

The potentiodynamic polarization plots of Q235 steel in SCPS at different chloride and pH values is presented in Figure 4. As the chloride concentration is increased, the OCP was decreased. At a pH of 13 and chloride concentration of 0.1M, the pitting potential decreased from 0.6V to approximately 0V. When the potential reaches the pitting potential, the current will increase rapidly resulting in rupture of the passive film and the formation of corrosion pits. When the chloride concentration is further increased, the range of the passive region is reduced, the pitting potential is lower and the current density before breakdown of the passive film is larger. The stability of the passive film is also reduced. When the pH was 12.5 and chloride concentration 0.05M, the pitting potential decreased from 1.0V to 0.5V. When pH was 11 and the chloride concentration 0.01M, no passive region is apparent on the polarization curve. This resulted in severe corrosion on Q235 steel through being unable to generate a passive film on the steel surface. In the simulated concrete pore solutions at pH 13 and 12.5, the Q235 steel still has an obvious passivation zone when the chloride concentration is 0.01M or higher. In the simulated concrete pore solution at pH 11, there is no passivation zone when the chloride concentration is 0.01 M.

The critical chloride concentration for pitting corrosion decreases as the pH decrease[24]. It shows that as the pH value decreases, the alkalinity of the simulated concrete pore solution decreases, the passive film will corrode at a lower chloride concentration, and the ability of the passive film to resist chloride decreases. In the simulated concrete pore solution with higher pH, the passive film is more stable.

#### 4. CONCLUSION

The passivation and corrosion behavior of Q235 steel in simulated concrete pore solution with different chloride concentrations and pH values was studied. The following conclusions are readily apparent from the present study:

1. Q235 steel shows n-type semiconductor behavior in simulated concrete pore solution. There are two different donor densities at pH 13 with the second slope potentially due to a deep donor level of the passive film. As the chloride concentration is increased the donor density also increases. The disorder and quantity of impurities in the passive film also rise.

2. With the increase of chloride concentration,  $R_{ct}$  will decrease indicating that the corrosion resistance of the passive film is reduced. Values of  $Q_f$  and  $Q_{dl}$  are increased due to the thinning or cracking of the passive film layer and corrosion caused by chloride present.

3. As pH decreases, the alkalinity of the simulated concrete pore solution will also decrease. The passive film will corrode locally at a lower chloride concentration and the ability of the passive film to resist chloride will be decreased. Q235 steel could not generate a passive film in the simulated concrete pore solution at a chloride concentration of 0.01M at pH 11, or at pH 9.

#### ACKNOWLEDGEMENTS

This work was supported by National key R & D Program (2018YFC0407102) and National Natural Science Foundation of China (No. 51871164).

#### References

1. C. Ivana, P. Ivana and S. Michael, *Corros. Sci.*, 48(2006)980.
2. C. L. Page and K. Treadaway, *Nature*, 297(1980)109.
3. M. Sanchez-Moreno, H. Takenouti, J. J. Garcia-Jareno, F. Vicente and C. Alonso, *Electrochim. Acta*, 54(2009)7222.
4. K. K. Sagoe-Crentsil, F. P. Glasser and J. T. S. Irvine, *Br. Corros. J.*, 27(2014)113.
5. B. Huet, V. L'Hostis, F. Miserque and H. Idrissi, *Electrochim. Acta*, 51(2005)172.
6. Y. S. Choi, S. T. Yi, M. Y. Kim, W. Y. Jung and E. I. Yang, *Constr. Build. Mater.*, 54(2014)180.
7. B. Yu, L. F. Yang, M. Wu and B. Li, *Constr. Build. Mater.*, 54(2014)385.
8. I. Khan, R. Francois and A. Castel, *Cem. Concr. Res.*, 56(2014)84.
9. G. S. Duffo, M. Reinoso, C. P. Ramos and S. B. Farina, *Cem. Concr. Res.*, 42(2012)111.
10. X. J. Zhu, Z. Z. Meng, Y. Liu, L. Xu and Z. X. Chen, *Adv. Mater. Sci. Eng.*, 3(2018)1.
11. H. Yu, K. K. Chiang and L. Yang, *Constr. Build. Mater.*, 26(2012)723.

12. X. Zhu, G. Zi, W. Lee, S. Kim and J. Kong, *Constr. Build. Mater.*, 124(2016)667.
13. J. Williamson and O. B. Isgor, *Corros. Sci.*, 106(2016)82.
14. M. Sanchez, J. Gregori, M. C. Alonso, J. J. Gaecia-Jareno and F. Vicente, *Electrochim. Acta*, 52(2006)47.
15. M. H. Dean and U. Stimming, *J. Electroanal. Chem. Interfacial Electrochem.*, 228(1987)135.
16. Z. H. Dong, W. Shi, G. A. Zhang and X. P. Guo, *Electrochim. Acta*, 56(2011)5890
17. L. Hamadou, A. Kadri and N. Benbrahim, *Appl. Surf. Sci.*, 252(2005)1510.
18. H. B. Gunay, P. Ghods, O. B. Isgor, G. J. C. Carpenter and X. H. Wu, *Appl. Surf. Sci.*, 274(2013)195.
19. D. D. Macdonald, *J. Electrochem. Soc.*, 139(1992)3434.
20. Y. F. Cheng and J. L. Luo, *Appl. Surf. Sci.*, 167(2000)113.
21. A. I. Munoz, J. G. Anton, J. L. Guinon and V. P. Herranz, *Corros. Sci.*, 48(2006)3349.
22. F. J. Tang, X. M. Cheng, G. Chen, R. K. Brow, J. S. Volz and M. L. Koenigstein, *Electrochim. Acta*, 92(2013)36.
23. J. J. Shi, D. Q. Wang, J. Ming and W. Sun, *J. Mater. Civ. Eng.*, 30(2018)1.
24. B. Lin, Y. Zuo, Y. M. Tang, X. H. Zhao and P. Rostron, *Int. J. Electrochem. Sci.*, 14(2019)3081.

© 2022 The Authors. Published by ESG ([www.electrochemsci.org](http://www.electrochemsci.org)). This article is an open access article distributed under the terms and conditions of the Creative Commons Attribution license (<http://creativecommons.org/licenses/by/4.0/>).